Andreas Hirsch, Michael Brettreich

Fullerenes

Chemistry and Reactions

WILEY-VCH Verlag GmbH & Co. KGaA

Andreas Hirsch
Michael Brettreich
Fullerenes

Further Reading from WILEY-VCH

S. Reich, C. Thomsen, J. Maultzsch

Carbon Nanotubes

2004
ISBN 3-527-40386-8

C. N. R. Rao, A. Müller, A. K. Cheetham (Eds.)

The Chemistry of Nanomaterials
2 Volumes

2004
ISBN 3-527-30686-2

A. de Meijere, F. Diederich (Eds.)

Metal-Catalyzed Cross-Coupling Reactions
Second Edition, 2 Volumes

2004
ISBN 3-527-30518-1

R. Mahrwald (Ed.)

Modern Aldol Reactions
2 Volumes

2004
ISBN 3-527-30714-1

Andreas Hirsch, Michael Brettreich

Fullerenes

Chemistry and Reactions

WILEY-VCH Verlag GmbH & Co. KGaA

Authors:

Prof. Dr. Andreas Hirsch
Dr. Michael Brettreich

Department of Organic Chemistry
Friedrich Alexander University
of Erlangen-Nuremberg
Henkestrasse 42
91054 Erlangen
Germany

All books published by Wiley-VCH are carefully produced. Nevertheless, authors, editors, and publisher do not warrant the information contained in these books, including this book, to be free of errors. Readers are advised to keep in mind that statements, data, illustrations, procedural details or other items may inadvertently be inaccurate.

Library of Congress Card No.: Applied for

British Library Cataloging-in-Publication Data:
A catalogue record for this book is available from the British Library.

Bibliographic information published by Die Deutsche Bibliothek
Die Deutsche Bibliothek lists this publication in the Deutsche Nationalbibliografie; detailed bibliographic data is available in the internet at http://dnb.ddb.de.

© 2005 Wiley-VCH Verlag GmbH & Co. KGaA, Weinheim

All rights reserved (including those of translation in other languages). No part of this book may be reproduced in any form – by photoprinting, microfilm, or any other means – nor transmitted or translated into a machine language without written permission from the publishers. Registered names, trademarks, etc. used in this book, even when not specifically marked as such, are not to be considered unprotected by law.

Printed in the Federal Republic of Germany
Printed on acid-free paper

Typesetting Manuela Treindl, Laaber
Printing Strauss GmbH, Mörlenbach
Bookbinding Litges & Dopf Buchbinderei GmbH, Heppenheim

ISBN 3-527-30820-2

Foreword

Ten years ago Prof. Andreas Hirsch, then finishing his "Habilitation" (an advanced junior research academic rank used in some European countries) in Prof. Hanack's laboratories in Tübingen, wrote THE seminal book about fullerene chemistry: "*The Chemistry of the Fullerenes*". This book, in our group, has many yellowed pages and an abundance of fingerprints, attesting to its outstanding usefulness as a reference book, or, better, a manual. The book has nine chapters covered in 203 pages, including an index.

In the intervening decade, though it would appear to some chemists in the world that the field of fullerene science had "matured", the current version of the book proves otherwise. In "*Fullerenes – Chemistry and Reactions*" Professor Hirsch has expanded the original 9 chapters to 14. The new chapters cover halogenation (Chap. 9), regiochemistry (Chap. 10), cluster modified fullerenes (Chap. 11), heterofullerenes (Chap. 12) and higher fullerenes (Chap. 13). The book is now 419 pages long, over double the number of the original book! The last three chapters give a strong impression that the field of fullerene chemistry is still vibrant and replete with challenges. Upon perusing its content, it is obvious that this book will be equally, or more, useful than its antecedent.

The statement I made on the back cover of "*The Chemistry of the Fullerenes*" applies today to "*Fullerenes – Chemistry and Reactions*" with only very minor changes that took place with time:

> "Though the synthetic fullerenes have been with us for only three years, the scientific articles based on them number in the thousands. It is therefore important and necessary to have a source of information which summarizes the most important and fundamental aspects of the *organic and organometallic chemistry* of the fullerenes. Dr. Hirsch is already well known for his important contributions to the field and is uniquely qualified to write what will become the *primary source* of information for the practicing organic and organometallic chemist.
>
> This book is logically arranged and information is easy to retrieve. The style lends itself to effortless reading and to learning more about the chemical properties of a family of molecules that constitute new building blocks for novel architectures in the still expanding universe of synthetic chemistry.
>
> This book will not only be found in university libraries but also on bookshelves of chemists interested in the art and science of structure and property manipulation by synthesis. Dr. Hirsch's *"The Chemistry of the Fullerenes"* is a

genuine, single author book. It is the first, and so far the best, monograph in the field. It stands out because its quality surpasses that of other multi-author compendia, that preceded it."

September 2004 *Fred Wudl*

Preface

It has now been more the ten years after the *The Chemistry of the Fullerenes* was published in 1994 by Thieme. This book became a classic in the field and was the major source of information summarizing the fundamental aspects of organic and organometallic chemistry of fullerenes. In the meantime many new achievements in fullerene chemistry were accomplished. For example, unprecedented exohedral addition reactions have been discovered and the knowledge how to design functionalized mono- and multiple adducts in a selective manner has continuously increased. New types of fullerene derivatives such as heterofullerenes and cluster modified fullerenes capable of entrapping small guest molecules have been made available for the first time. Thanks to the developments in preparative fullerene chemistry the performance of highly sophisticated derivatives was steadily improved leading to systems with remarkable biological and materials properties. Fullerene chemistry continues to excite. So it came as no surprise that the discovery of the fullerenes by Curl, Kroto and Smalley was rewarded with the Noble prize in 1996.

Within the last years I was repeatedly asked by friends and colleagues: When will you present the second edition? Of course the demand for an updated book was obvious. However, I hesitated to take action because it was clear that preparing an update means more or less writing a new book. Then about two years ago after Wiley-VCH took over the Chemistry monographs of Thieme I had a nice conversation with Elke Maase from Wiley-VCH who finally convinced me to write the second edition. I could not resist any longer. But I needed help. Due to the many new achievements in the field there was no doubt to me that updating the field of fullerene chemistry in a reasonable time is only possible if I would find a co-author. I was very happy that I could convince Michael Brettreich to participate in this exciting project and become the co-author. Michael Brettreichs accomplishments in synthetic and supramolecular fullerene chemistry are outstanding and he was the best person I could think of to work with me on the book.

Just by comparing the number of publications on fullerenes (5500 until 1994 and 21500 between 1994 and now) it was immediately clear that the whole literature even that focussing on fullerene chemistry cannot be covered in a single monograph. We had to carefully select and condense the material, refer to the many excellent reviews of specific subjects such as chemistry of higher fullerenes and supramolecular chemistry of fullerenes.

Also fascinating developments in various fields of applications such as opto-electronic-, materials- and medical applications are just barely touched. Our main intention was to put the focus on molecular fullerene chemistry.

Compared to *The Chemistry of the Fullerenes* of 1994 the content as determined from the number of pages was more than doubled. The predecessor served as a good basis for Chapters 1 to 8 which are *The Parent Fullerenes*, *Reduction*, *Nucleophilic Additions*, *Cycloadditions*, *Hydrogenation*, *Radical Additions*, *Transition Metal Complex Formation* as well as *Oxidation and Reactions with Electrophiles*. However, an enormous amount of new material needed to be included making some of these chapters, especially Chapter 3: *Nucleophilic Additions*, Chapter 4: *Cycloadditions* and Chapter 7: *Transition Metal Complex Formation* to appear in new light. Moreover, four completely new chapters needed to be added because of recent ground breaking developments. These are Chapter 10: *Regiochemistry of Multiple Additions*, Chapter 11: *Cluster Modified Fullerenes*, Chapter 12: *Heterofullerenes* and Chapter 13: *Chemistry of Higher fullerenes*. Moreover *Halogenation* which was part of Chapter 8: *Oxidation and Reactions of Electrophiles*, is now presented independently in Chapter 9, because of very fruitful accomplishments in this area. The final Chapter: *Principles and Perspectives of Fullerene Chemistry* (now Chapter 14) was also heavily rearranged and extended, for example, by the comparison of exohedral- and endohedral reactivity as well as detailed analysis of structural aspects and aromaticity of fullerenes. Finally, the entire artwork, especially the drawing of the molecules in schemes and figures was improved considerably. As a consequence, what we present now is indeed a new book, which is also expressed by changing the title to *Fullerenes – Chemistry and Reactions*.

The authors would like to acknowledge a number of persons, who were very important to us during the process of writing the book. We thank Christian Hub and Dr. Otto Vostrowsky for their help with preparing formulas, schemes and other art work. We also thank Prof. Dr. Olga Boltalina, Dr. Otto Vostrowsky, Dr. Nicos Chronakis and Irene Brettreich for proof reading of the manuscript. It was a major relief that Erna Erhardt continuously assisted us in organizing the referencing and in the preparation of tables. The beautiful cover picture was designed by Adrian Jung. Thank you very much. From Wiley-VCH we thank Elke Maase for the excellent collaboration. We also thank her and many colleagues from the fullerene community for motivating us to write this book. Our specials thanks go to our wives and families for their enormous patience.

Erlangen
August 2004

Andreas Hirsch

Preface of "The Chemistry of the Fullerenes" by Andreas Hirsch (1994)

"Buckminsterfullerene: Is it a real thing?" This question was in our heads that evening in November 1990, when Fred Wudl came into the lab and showed us the first 50 mg sample of C_{60}. Although at that time there was evidence for the geometrical structures of this soccer ball shaped molecule and his bigger brother the "American football" C_{70}, no one knew what the chemical and physical properties of these fascinating molecular allotropes of carbon would be. On that same night we started to work on C_{60} and three reversible one electron reductions of the carbon sphere were found – one more than already detected by the Rice group. We were all enthusiastic and Fred projected possible chemical transformations and proposed remarkable electronic properties of fulleride salts – a prediction that shortly thereafter became reality by the discovery of the superconductivity of K_3C_{60} in the Bell labs. It was one of the greatest opportunities in my scientific life, that Fred asked me to participate in the ball game and to investigate organic fullerene chemistry. He also encouraged me to carry on this work in Germany, once I had finished my postdoctoral time in his group in Santa Barbara. The pioneering research of these early days is still a basis of my present work. Fullerene chemistry, which is unique in many respects, has meanwhile exploded. In a very short period of time a huge number of chemical transformations of the "real thing" C_{60} and outstanding properties of fullerene derivatives have been discovered. Many principles of fullerene chemistry are understood. The fullerenes are now an established compound class in organic chemistry.

It is therefore the right time to give a first comprehensive overview of fullerene chemistry, which is the aim of this book. This summary addresses chemists, material scientists and a broad readership in industry and the scientific community. The number of publications in this field meanwhile gains such dimensions that for nonspecialists it is very difficult to obtain a facile access to the topics of interest. In this book, which contains the complete important literature, the reader will find all aspects of fullerene chemistry as well as the properties of fullerene derivatives. After a short description of the discovery of the fullerenes all methods of the production and isolation of the parent fullerenes and endohedrals are discussed in detail (Chapter 1). In this first chapter the mechanism of the fullerene formation, the physical properties, for example the molecular structure, the thermodynamic, electronic and spectroscopic properties as well as solubilities are also summarized. This knowledge is necessary to understand the chemical behavior of the fullerenes.

The description of the chemistry of the fullerenes themselves is organized according to the type of chemical transformation, starting from the reduction (Chapter 2), nucleophilic additions (Chapter 3), cycloadditions (Chapter 4), hydrogenation (Chapter 5), radical additions (Chapter 6), transition metal complex formation (Chapter 7) through oxidation and reactions with electrophiles (Chapter 8). Most of the examples presented in these chapters are reactions with C_{60}, since only very little work has been published on C_{70} and the higher fullerenes. It is the aim to provide an understanding of the basic characteristics of fullerene chemistry. This is achieved by a comparative description of both experimental and theoretical investigations in each of these chapters. It is also emphasized in each chapter wherever a reaction type leads to a fullerene derivative with a potential for practical application. In the last chapter (Chapter 9) the emerging principles of fullerene chemistry, such as reactivity and regiochemistry, are evaluated and summarized. The fullerene chemistry is still in an early stage of development. For synthetic chemists a lot of challenging work remains to be done. A prediction of the future directions of fullerene chemistry is therefore also given in Chapter 9 and finally, since from the beginning of the fullerene era many practical uses have been proposed, perspectives for applications are evaluated.

Writing this book prevented me for some time from carrying out practical work with my own hands. Nevertheless, since I have had co-workers like Thomas Grösser, Iris Lamparth, Andreas Skiebe and Antonio Soi, the experimental work on fullerenes in my lab has proceeded, even with much success. I am also indebted to my co-workers for their assistance in preparing figures and illustrations presented in this book. I thank Dr. L. R. Subramanian for reading the entire manuscript and for useful suggestions.

I thank Dr. J. P. Richmond for the excellent co-operation, which enabled the fast realization of this book project.

I am very grateful to my teacher Prof. Dr. Dr. h. c. M. Hanack, who has been supporting me for many years and who provided the starting conditions for writing this book.

It was Prof. Dr. F. Wudl who introduced me to the art of fullerene chemistry and who inspired me to continue with this work, for which I want to thank him very much. On reviewing the manuscript he came up with cogent comments and suggestions.

My special thanks go to my wife Almut, who, despite the fact that for several months she was very often deprived of the company of her husband, responded with warmth and understanding.

Tübingen, May 1994 *Andreas Hirsch*

Contents

Abbreviations

a.u.	arbitrary units
AIBN	2,2′-azobisisobutyronitril
ALS	amyotrophic lateral sclerosis
APCI	atmospheric pressure chemical ionization
ATP	adenosintriphosphate
BN	boron nitride
BP	biphenyl
BtOH	1H-benzotriazol
CD	circular dichroism
CI	chemical ionization
CSA	camphor sulfonic acid
CT	charge transfer
CV	cyclic voltammetry
CVM	chemical vapor modification
DABCO	1,4-diazabicyclo[2.2.2]octane
DBU	1,8-diazabicyclo[5.4.0]undec-7-ene
DCC	N,N′-dicyclohexylcarbodiimide
DCI	desorptive chemical ionization
DDQ	2,3-dichloro-5,6-dicyanobenzoquinone
DFT	density functional theory
DIBAL-H	diisobutylaluminium-hydride
DIOP	2,3-O-isopropylidene-2,3-dihydroxy-1,4-bis(diphenylphosphanyl)butane
DMA	9,10-dimethylanthracene
DMAD	dimethylacetylenedicarboxylate
DMAP	4-(dimethylamino)pyridine
DMB	dimethoxybenzene
DMF	dimethylformamide
DMSO	dimethylsulfoxide
DNA	desoxyribonucleid acid
DOS	density of states
DPIF	1,3-diphenylisobenzofurane
dppb	1,2-bis(diphenylphosphino)benzene
DPPC	dipalmitoylphosphatidylcholine

dppe	1,2-bis(diphenylphosphino)ethane
dppf	1,1′-bis(diphenylphosphino)-ferrocene
DSC	digital scanning calorimetry
EDCI	N′-(3′-dimethylaminopropyl)-N-ethylcarbodiimide hydrochloride
EI	electron impact
EPR	electron paramagnetic resonance
ESCA	electron spectroscopy for chemical analysis
ESR	electron spin resonance
FAB	fast atom bombardment
FD	field desorption
FT-ICR	fourier transform ion cyclotron resonance
FVP	flash-vacuum pyrolysis
GPC	gel permeation chromatography
HETCOR	heteronuclear chemical shift correlation
HIV	human immunodeficiency virus
HMPA	hexamethyl phosphoric acid
HOMO	highest occupied molecular orbital
HPLC	high pressure liquid chromatography
IC	ion chromatography
ICR	ion cyclotron resonance
INADEQUATE	incredible natural abundance double quantum transition experiment
IPR	isolated pentagon rule
IR	infrared
ITO	indium-tin-oxide
LB	Langmuir-Blodgett
LDA	Lithium diisopropylamide
LESR	light-induced ESR measurement
LUMO	lowest unoccupied molecular orbital
MALDI	matrix-assisted laser desorption ionization
MCPBA	m-chloroperoxybenzoic acid
MEM	methoxy ethoxy methyl
MO	molecular orbital
MRI	magnetic resonance imaging
MS	mass spectrometry
NCS	N-chlorosuccinimide
NICS	nucleus-independent chemical shift
NIR	near infrared
NMA^+	N-methylacridinium-hexafluorophosphate
NMR	nuclear magnetic resonance
ODCB	ortho-dichlorobenzene
OL	optical limiting
PAH	polycyclic aromatic hydrocarbon
PCBA	[6,6]-phenyl-C_{61}-butyric acid

PCC	pyridinium chlorochromate
PET	photoinduced electron transfer
POAV	π orbital axis vector
POM	polarizing optical microscopy
PPV	poly-para-phenylen-vinylene
PVK	poly(N-vinylcarbazole)
QCM	quartz crystal microbalance
RE	resonance energy
RETOF	reflectron time of flight
SAM	self-assembled monolayer
SEC	size-exclusion chromatography
SET	single electron transfer
SWNT	single-walled carbon nanotube
TBA	tetrabutylammonium
TCE	trichloroethylene
TCNE	tetracyanoethylene
TCNQ	tetracyano-p-quinodimethane
TDAE	tetrakis(dimethylamino)ethylene
TEMPO	2,2,6,6-tetramethylpiperidin-1-yloxyl
TFA	trifluoroacetic acid
TGA	thermal gravimetric analysis
THA	tetrahexylammonium
THF	tetrahydrofuran
TMEDA	N,N,N′,N′-tetramethylene diamine
TMM	trimethylenemethane
TOF	time of flight
TosOH	4-toluenesulfonic acid
TPP	tetraphenylporphyrin
TPP^+	triphenylpyriliumtetrafluoroborate
TTF	tetrathiafulvalene
UHV-STM	ultra-high vacuum scanning tunneling microscopy
UV	ultraviolet
UV/Vis	ultraviolet/visible
VB	valence bond
Vis	visible
XPS	X-ray photoelectron spectroscopy

1
Parent Fullerenes

1.1
Fullerenes: Molecular Allotropes of Carbon

For synthetic chemists, who are interested in the transformation of known and the creation of new matter, elemental carbon as starting material once played a minor role. This situation changed dramatically when the family of carbon allotropes consisting of the classical forms graphite and diamond became enriched by the fullerenes. In contrast to graphite and diamond, with extended solid state structures, fullerenes are spherical molecules and are soluble in various organic solvents, an important requirement for chemical manipulations.

Fullerenes are built up of fused pentagons and hexagons. The pentagons, absent in graphite, provide curvature. The smallest stable, and also the most abundant fullerene, obtained by usual preparation methods is the I_h-symmetrical Buckminsterfullerene C_{60} (Figure 1.1). Buckminsterfullerene has the shape of a soccer ball. The next stable homologue is C_{70} (Figure 1.2) followed by the higher fullerenes C_{74}, C_{76}, C_{78}, C_{80}, C_{82}, C_{84}, and so on. The building principle of the fullerenes is a consequence of the Euler theorem, which says that for the closure of each spherical network of n hexagons, 12 pentagons are required, with the exception of $n = 1$.

Compared to small two-dimensional molecules, for example the planar benzene, the structures of these three-dimensional systems are aesthetically appealing. The beauty and the unprecedented spherical architecture of these molecular cages immediately attracted the attention of many scientists. Indeed, Buckminsterfullerene C_{60} rapidly became one of the most intensively investigated molecules. For synthetic chemists the challenge arose to synthesize exohedrally modified derivatives, in which the properties of fullerenes can be combined with those of other classes of materials. The following initial questions concerned the derivatization of fullerenes: What kind of reactivity do the fullerenes have? Do they behave like a three-dimensional "superbenzene"? What are the structures of exohedral fullerene derivatives and how stable are they?

The IUPAC method of naming Buckminsterfullerene given below is too lengthy and complicated for general use [1]:

Hentriacontacyclo[29.29.0.0.^{2,14}.0^{3,12}.0^{4,59}.0^{5,10}.0^{6,58}.0^{7,55}.0^{8,53}.0^{9,21}.0^{11,20}.0^{13,18}.0^{15,30}.0^{16,28}.0^{17,25}.0^{19,24}.0^{22,52}.0^{23,50}.0^{26,49}.0^{27,47}.0^{29,45}.0^{32,44}.0^{33,60}.0^{34,57}.0^{35,43}.0^{36,56}.0^{37,41}.0^{38,54}.0^{39,51}.0^{40,48}.0^{42,46}]hexaconta-1,3,5(10),6,8,11,13(18),14,16,19,21,23,25,27,

29(45),30,32,(44),33,35(43),36,38(54),39(51),40(48),41,46,49,52,55,57,59-triacontaene.

Furthermore, the enormous number of derivatives, including the multitude of possible regioisomers, available by chemical modifications requires the introduction of a simple nomenclature. According to the latest recommendation, the icosahedral Buckminsterfullerene C_{60} was named as (C_{60}-I_h)[5,6]fullerene and its higher homologue C_{70} as (C_{70}-D_{5h})[5,6]fullerene [2, 3]. The parenthetical prefix gives the number of C-atoms and the point group symbol; the numbers in brackets indicate the ring sizes in the fullerenes. Fullerenes involving rings other then pentagons and hexagons are conceptually possible (*quasi*-fullerenes [4]). The identification of a well defined and preferably contiguous helical numbering pathway is the basis for the numbering of C-atoms within a fullerene. Such a numbering system is important for the unambiguous description of the multitude of possible regioisomeric derivatives formed by exohedral addition reactions. A set of rules for the atom numbering in fullerenes has been adopted [2, 3]. The leading rule (Fu-3.1.1) is:

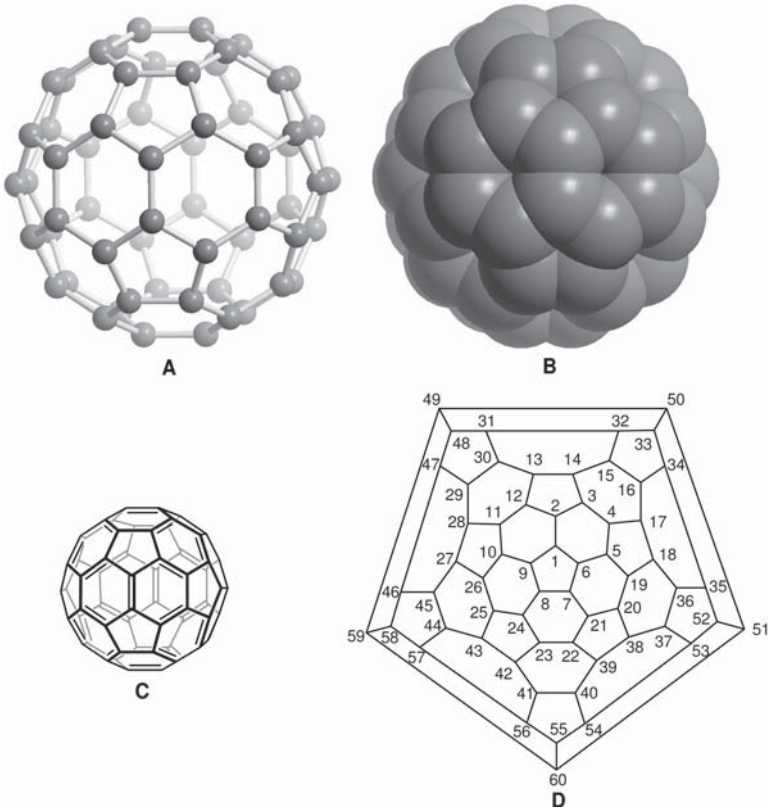

Figure 1.1 Schematic representations of C_{60}. (A) ball and stick model, (B) space filling model, (C) VB formula, (D) Schlegel diagram with numbering of the C-atoms (according to [4]).

Proper rotation axes (C_n) are examined in sequence from the highest-order to the lowest-order axis, until at least one contiguous helical pathway is found that begins in a ring through which a proper rotation axis passes, at the end a bond bisected by a proper rotation axis, or at an atom through which a proper rotation axis passes. Numbering begins at the end of such a contiguous helical pathway, and the corresponding axis is called the "reference axis".

This system allows also for the indication of the absolute configuration of inherently chiral fullerenes by introducing the stereodescriptors (^{f,s}C) and (^{f,s}A) ("f" = fullerene; "s" = systematic numbering; "C" = clockwise; "A" = anti-clockwise).

In another nomenclature recommendation it was suggested that fullerenes be named in the same way as annulenes, for which the number of C-atoms is indicated in square brackets in front of the word [4]. For fullerenes the number of C-atoms is accompanied by the point group symmetry and by the number of the isomer (using capital Roman) in cases were there are more than one. This is especially important for higher fullerenes. Thus, for Buckminsterfullerene the full description is

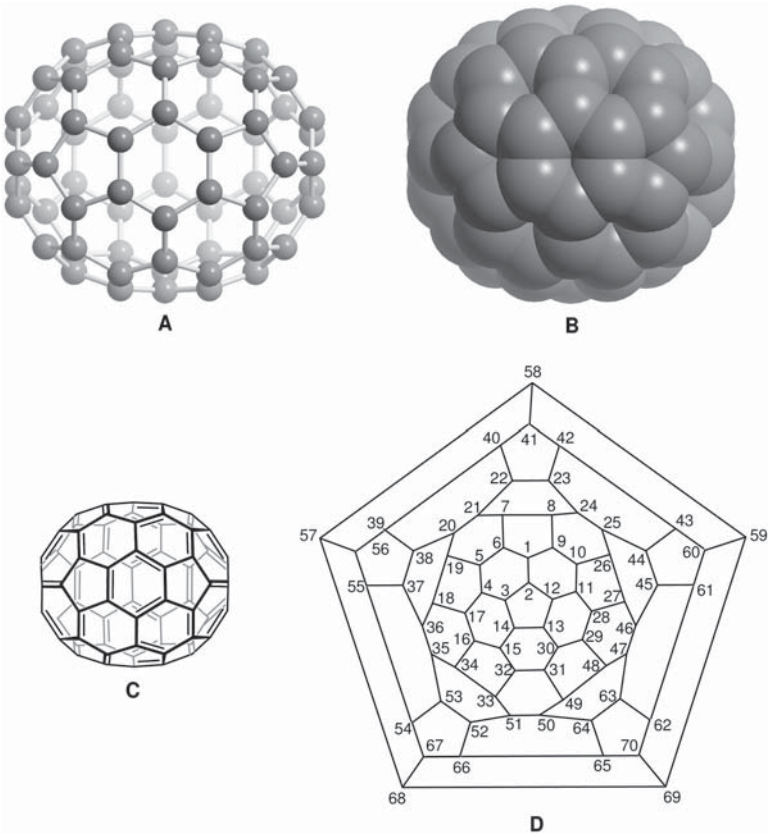

Figure 1.2 Schematic representations of C_{70}. (A) ball and stick model, (B) space filling model, (C) VB formula, (D) Schlegel diagram with numbering of the C-atoms (according to [4]).

[60-I_h]fullerene and for C_{70} (Figure 1.2) [70-D_{5h}]fullerene. In most cases further simplification to [60]fullerene and [70]fullerene or even C_{60} and C_{70} is made, since there are no other stable isomers of these fullerenes. An alternative numbering of C-atoms to that pointed out above [2, 3] is also based on a contiguous spiral fashion but numbers the bond of highest reactivity as 1,2 (Figure 1.1) [4]. For [60]fullerene these are the bonds at the junction of two hexagons ([6,6]-bonds). Since the chemistry of [70]fullerene has many similarities to that of [60]fullerene, it is advantageous if the numbering scheme for [70]fullerene parallels that of [60]fullerenes, which is indeed possible (Figure 1.2) [4].

Valence bond (VB) formulas or Schlegel diagrams are useful for simple schematic representations of fullerenes and their derivatives. VB formulas are mostly used for parent fullerenes or for derivatives with a few modifications of the cage structure only. A Schlegel diagram shows each C-atom of the fullerene, which is flattened out in two dimensions. This model is suitable for considering polyadducts, for example, polyhydrofullerenes.

The main type of chemical fullerene derivatizations are addition reactions. Regardless of the relatively many possible reaction sites, addition reactions show a remarkable regioselectivity, especially when the number of addends is small. This is another fulfilled requirement, which makes these molecular spheres exciting objects for synthetic chemists.

1.2 Discovery of the Fullerenes

In 1966 Deadalus alias D. E. H. Jones considered the possibility of making large hollow carbon cages, structures now called giant fullerenes [5, 6]. This suggestion elicited no reaction from the scientific community. Four years later, in 1970, simulated by the synthesis of the bowl shaped corannulene **1** [7], Osawa first proposed the spherical I_h-symmetric football structure for the C_{60} molecule (**2**) [8, 9]. During his efforts to find new three-dimensional superaromatic π-systems, he recognized corannulene to be a part of the football framework. Subsequently, some theoretical papers of other groups appeared, in which inter alia Hückel calculations on C_{60} were reported [10–13].

1

2

In 1984 it was observed that, upon laser vaporization of graphite, large carbon-only clusters C_n with $n = 30–190$ can be produced [14]. The mass distribution of these clusters was determined by time-of-flight mass spectrometry. Only ions with

even numbers of carbon atoms were observable in the spectra of large carbon clusters ($n \geq 30$). Although C_{60} and C_{70} were among these clusters, their identity was not recognized. The breakthrough in the experimental discovery of the fullerenes came in 1985 [15] when Kroto visited the Rice University in Houston. Here, Smalley and co-workers developed a technique [16] for studying refractory clusters by mass spectrometry, generated in a plasma by focusing a pulsed laser on a solid, in this case graphite. Kroto and Smalley's original goal was to simulate the conditions under which carbon nucleates in the atmospheres of red giant stars. Indeed, the cluster beam studies showed that the formation of species such as the cyanopolyynes HC_7N and HC_9N, which have been detected in space [17, 18], can be simulated by laboratory experiments [19]. These studies found that, under specific clustering conditions, the 720 mass peak attributed to C_{60}, and to a lesser extent the peak attributed to C_{70}, exhibits a pronounced intensity in the spectra (Figure 1.3). Conditions could be found for which the mass spectra were completely dominated by the C_{60} signal. Kroto and Smalley immediately drew the right conclusion of these experimental findings. The extra stability of C_{60} is due to its spherical structure, which is that of a truncated icosahedron with I_h symmetry [15]. This molecule was named after the architect Buckminster Fuller, whose geodesic domes obey similar building principles. Retrospectively, the enhanced intensity of the peak of C_{70}, which is also a stable fullerene, became understandable as well. Although Buckminsterfullerene (C_{60}) was discovered, a method for its synthesis in macroscopic amounts was needed.

This second breakthrough in fullerene research was achieved by Krätschmer and Huffman [20]. Their intention was to produce laboratory analogues of interstellar dust by vaporization of graphite rods in a helium atmosphere [21]. They observed that, upon choosing the right helium pressure, the IR-spectrum of the soot, generated by the graphite vaporization, shows four sharp stronger absorptions,

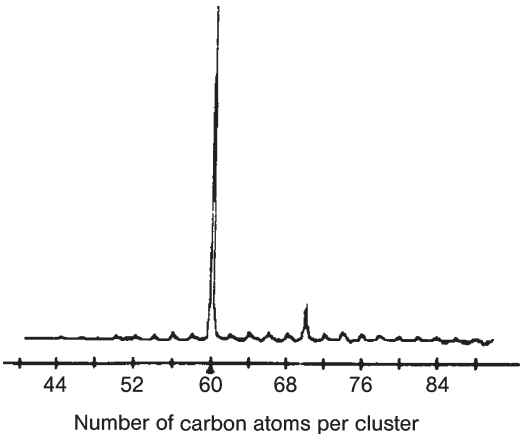

Figure 1.3 Time-of-flight mass spectrum of carbon clusters produced by laser vaporization of graphite under the optimum conditions for observation of a dominant C_{60} signal [15].

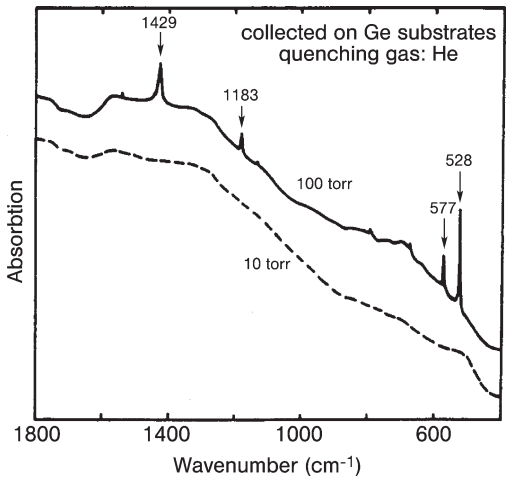

Figure 1.4 IR-spectra of soot particles produced by evaporation of graphite under different helium quenching gas pressures. The occurrence of the four additional sharp peaks at elevated helium pressures turned out to originate from [60-I_h]fullerene (C_{60}) [20].

together with those of the continuum of regular soot (Figure 1.4) [22]. These absorptions were close to the positions predicted by theory for Buckminsterfullerene [23]. The fullerenes were then isolated from the soot by sublimation or extraction with benzene. This allowed the verification of their identity by spectroscopic and crystallographic methods as well as by control experiments with ^{13}C-enriched material. Along with Buckminsterfullerene C_{60}, higher homologues are also obtained by this technique. Fullerenes were then available for the scientific community.

1.3 Fullerene Production

1.3.1 Fullerene Generation by Vaporization of Graphite

1.3.1.1 Resistive Heating of Graphite

Macroscopic quantities of fullerenes were first generated by resistive heating of graphite [20]. This method is based on the technique for the production of amorphous carbon films in a vacuum evaporator [24]. The apparatus (Figure 1.5) that Krätschmer and Fostiropoulos used for the first production of fullerenes consisted of a bell jar as recipient, connected to a pump system and a gas inlet. In the interior of the recipient two graphite rods are kept in contact by a soft spring. Thereby, one graphite rod is sharpened to a conical point, whereas the end of the other is flat. The graphite rods are connected to copper electrodes.

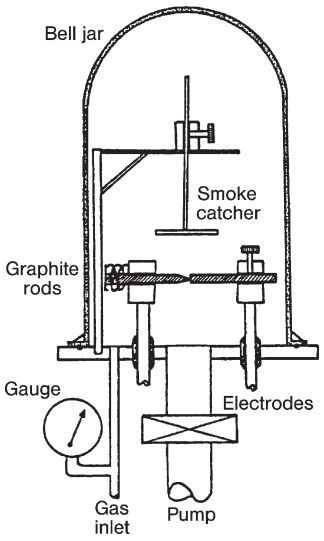

Figure 1.5 Fullerene generator originally used by Krätschmer [20].

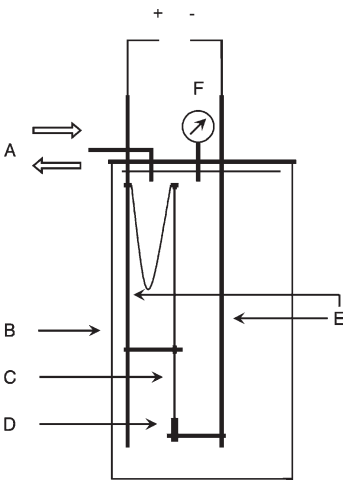

Figure 1.6 Simple benchtop reactor developed by Wudl [27]. Helium supply and connection to a vacuum system (A), Pyrex bell jar (B), graphite rod (3 mm) (C), graphite rod (12 mm) (D), copper electrode (E), manometer (F).

To produce soot, the apparatus is repeatedly evacuated and purged with helium and finally filled with about 140 mbar of helium. After applying a voltage, the electric current passing through the rods dissipates most of its Ohmic power heating at the narrow point of contact. This leads to a bright glowing in this area at 2500–3000 °C. Simultaneously, smoke develops at the contact zone, being transported away by convection and collected on the cooler areas (bell jar and smoke catcher) of the apparatus. The evaporation of the graphite is most efficient at the sharpened end of the rod. After the reaction is over, fullerenes are extracted from the soot, for example with toluene, in about 10–15% yield.

Modifications of this type of fullerene reactor are gravity feed generators [25–27]. The advantage of these generators is their simple construction principle. This, together with their low costs, makes them attractive for synthetic chemists. A schematic representation of such a simple benchtop reactor, developed by Wudl [27] is given in Figure 1.6. A thin graphite rod (3 mm), guided by a copper sleeve, with a sharpened tip is placed on a thick rod (12 mm). A commercially available arc welder serves as power supply. After applying a current (AC or DC) of about 40–60 A, only the material of the thin rod evaporates, whereupon it slips downward, guided by the copper sleeve that keeps the electrical contact. After a few minutes the rod is consumed to the point that it can not any longer make contact with the 12 mm rod. The power is then shut off. Based on evaporated graphite, fullerene yields of 5–10% are obtained [27, 28].

The buffer gas cools the plasma by collisions with the carbon vapor. The gas has to be inert, to prevent reactions with smaller carbon clusters or atoms, initially formed by the evaporation. Using N_2 dramatically reduces the yield of fullerenes, presumably due to nitrogen atoms, formed in the hot zone of the generator, reacting with the carbon fragments [28]. The highest yields of fullerenes are obtained if helium is used as buffer gas. Also, the concentration of the buffer gas is important (Figure 1.7), with maximum yields obtained between 140 and 160 mbar [28]. With a very low buffer gas pressure the carbon radicals diffuse far from the hot zone and the clusters continue to grow in an area that is too cool to allow an annealing to spherical carbon molecules. Conversely, if the pressure of the buffer gas is too high, a very high concentration of carbon radical results in the hot reaction zone. This leads to a fast growth of particles far beyond 60 C-atoms and the annealing process to fullerenes cannot compete [29].

During these resistive heating procedures the formation of slag, depositing on the thicker graphite rod, can be observed after some time of evaporation. As long as this vapor-deposited boundary layer remains between the two electrodes in a sufficiently thick and resistive form, the electrical power continues to be dissipated just in this small zone, and carbon vaporization from the end of the thin graphite rod proceeds efficiently [30]. Thus, the formation of such a resistive layer may be an important requirement for the continuation of smoke production. In the beginning of the reaction this was guaranteed by the sharpened thin graphite rod (heat dissipation in this small resistive zone). For graphite rods, with diameters of 6 mm or greater, the resistive layer does not remain sufficiently resistive and the entire length of the graphite rod eventually begins to glow. This causes inefficient evaporation of carbon from the center of the rod. Therefore, only comparatively thin graphite rods can be used for efficient fullerene production by the resistive heating technique.

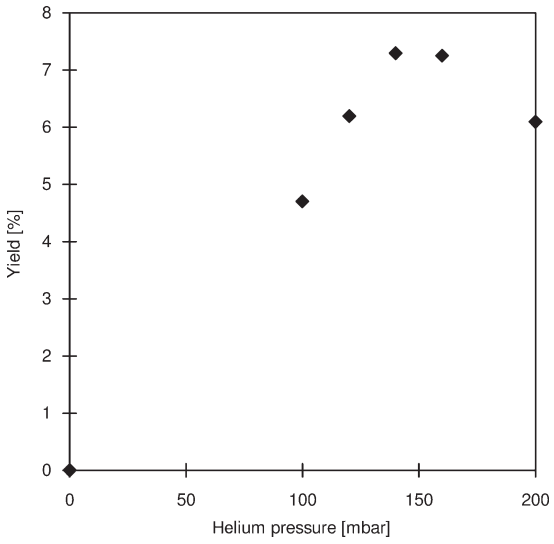

Figure 1.7 Dependence of the fullerene yield on the helium gas pressure in the fullerene generator.

1.3.1.2 Arc Heating of Graphite

An alternative to resistive heating is arc vaporization [29, 31–36] of graphite, first developed by Smalley [31]. If the tips of two sharpened graphite rods are kept in close proximity, but not in a direct contact, the bulk of the electrical power is dissipated in an arc and not in Ohmic heating. In an original generator a spring tension was adjusted to maintain the arc between the nearly contacting graphite electrodes. The most efficient operation occurs when the electrodes are barely touching, which lead to the term "contact-arcing" [31]. This method also allows an efficient evaporation of carbon with somewhat thicker, for example, 6 mm rods. The yield of fullerenes obtained by this technique was found to be about 15%. However, by increasing the rod diameter the yield decreases almost linearly [31], which also prevents an upscaling to very large rod sizes. The reason for the low yields observed by using larger rod-sizes is the fullerenes sensitivity towards UV-radiation. Very intense UV-radiation originates from the central portion of the arc plasma. Newly formed fullerenes moving from the region around the arc are exposed to this intense light flux. The absorption of UV-light produces a triplet state (T_1), which lives for a few microseconds (Scheme 1.1) [37].

$$C_{60}\,(S_0) + h\upsilon \rightarrow C_{60}{}^{*}\,(T_1)$$

Scheme 1.1

In this T_1 state the fullerene is an open shell system and very susceptible to other carbon species C_n. As a result of such a reaction a non-vaporizable insoluble product may be formed (Scheme 1.2) [30].

$$C_{60}{}^{*}\,(T_1) + C_n \rightarrow \text{insoluble carbon}$$

Scheme 1.2

The effect of increased rod sizes is a larger photochemically dangerous zone. The rate of migration of the newly formed fullerenes through this zone, however, remains constant. Therefore, the yield of fullerenes that migrate through this region without reacting with other carbon species linearly decreases with the rod diameter [30]. A mathematical model for an arc reactor has taken into account (a) cooling and mixing of carbon vapor with buffer gas, (b) non-isothermal kinetics of carbon cluster growth and (c) formation of soot particles and heterogeneous reactions at their surface. This model provided good coincidence of experimental and calculated values both for the fullerene yields and the C_{60}/C_{70} ratio in the reaction products obtained under widely varied conditions [38].

The ratio of C_{60} to higher fullerenes is typically about 8 : 2. The relative yields of higher fullerenes were improved when graphite containing light elements such as B, Si or Al was used and the buffer gas He was mixed with a small amount of N_2 [39, 40]. Fullerenes have also been synthesized by a pulse arc discharge of 50 Hz–10 kHz and 150–500 A, with graphite electrodes and ambient helium (about 80 torr). Instead of graphite, coal was also used as carbon source [41]. Extraction of the corresponding soot with toluene resulted in a 4–6% yield of fullerenes.

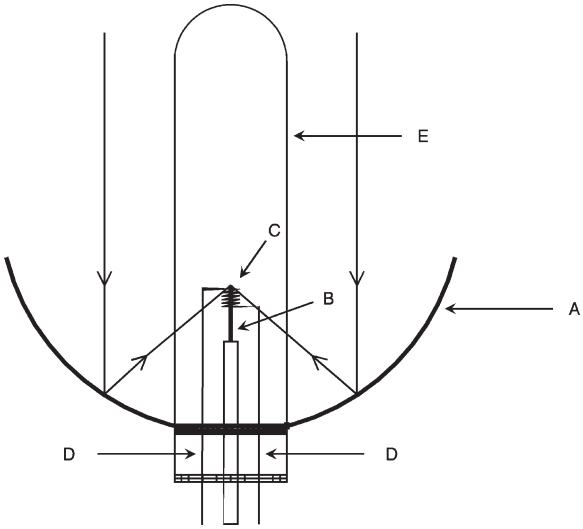

Figure 1.8 "Solar 1" fullerene generator [30].
(A) Parabolic mirror, (B) graphite target, (C) preheater,
(D) insulated preheater connectors and (E) glass tube.

1.3.1.3 Solar Generators

The problem of intense UV-radiation is avoided by the use of solar furnaces as fullerene generators [30, 42]. Although sun light is used to evaporate graphite the exposure of generated fullerenes to radiation is far less extensive than with resistive heating or arc vaporization techniques. As an example solar generator, "Solar 1" developed by Smalley [30] will be discussed (Figure 1.8). Sunlight is collected by parabolic mirrors and focused onto a tip of a graphite rod. This rod is mounted inside a Pyrex tube. To minimize conductive heat loss and to provide suitable conditions for the annealing process of the carbon clusters, the graphite rod was enclosed by a helical tungsten preheater. After degassing the system with the preheater, it is filled with about 50 Torr of argon and sealed off. To run the reaction the apparatus is adjusted so that the sunlight is focused directly onto the tip of the graphite target. The argon gas heated by the tungsten preheater is efficiently carried up over the solar-irradiated carbon tip by convection (solar flux: 800–900 W m^{-2}). The condensing carbon vapor quickly moves from the intensive sunlight, cools in the upper regions of the Pyrex tube and subsequently deposits on the upper walls. Although fullerenes can be obtained this way, the efficiency of the prototype "Solar-1" generator is not very high.

1.3.1.4 Inductive Heating of Graphite and Other Carbon Sources

Fullerenes can also be produced by direct inductive heating of a carbon sample held in a boron nitride support [43]. Evaporation at 2700 °C in a helium atmosphere affords fullerene-containing soot that is collected on the cold Pyrex glass of the reaction tube. This method allows a continuous operation by keeping the graphite

sample in the heating zone. Upon evaporating 1 g of graphite, 80 to 120 mg of fullerene extract can be obtained in 10 min.

Continuous production of fullerenes was possible by pyrolysis of acetylene vapor in a radio-frequency induction heated cylinder of glassy polymeric carbon having multiple holes through which the gas mixture passes [44]. Fullerene production is seen at temperatures not exceeding 1500 K. The yield of fullerenes, however, generated by this method is less than 1%. A more efficient synthesis (up to 4.1% yield) was carried out in an inductively coupled radio-frequency thermal plasma reactor [45].

1.3.2
Fullerene Synthesis in Combustion

The existence of fullerenes in sooting flames was first revealed by mass spectrometry studies [46, 47]. Also, the production of fullerenes in optimized sooting flames is possible [48–52]. For this purpose premixed laminar benzene–oxygen–argon flames have been operated under a range of conditions, including different pressures, temperatures and carbon-to-oxygen ratios. Along with fullerenes and soot, polyaromatic hydrocarbons (PAHs) are formed simultaneously. The yield of fullerenes, as well as the C_{70}:C_{60} ratio, strongly depends on the operation mode. The amount of C_{60} and C_{70}, produced under different sooting flame conditions is in the range 0.003–9% of the soot mass. Expressed as percentage of fuel carbon, the yields varies from $2 \cdot 10^{-4}$ to 0.3% for a non-sooting flame, obtained at optimum conditions, at a pressure of 20 Torr, a carbon-to-oxygen ratio of 0.995 with 10% argon and a flame temperature of about 1800 K. The C_{70}:C_{60} ratio varies from 0.26 to 5.7, which is much larger than that observed for graphite vaporization methods (0.02–0.18). This ratio tends to increase with increasing pressure [48].

Further optimization of the formation of fullerenes in combustion lead to the development of efficient pilot plants [53–56]. Currently, 400 kg of fullerenes per year (Mitsubishi's Frontier Carbon Corporation) are obtained by these methods. Ton scale production is expected in the near future. This remarkable development has allowed fullerenes to be sold for less than \$300 kg^{-1}, a sharp improvement on the \$ 40 000 kg^{-1} rate that prevailed not long ago [57].

1.3.3
Formation of Fullerenes by Pyrolysis of Hydrocarbons

Fullerenes can also be obtained by pyrolysis of hydrocarbons, preferably aromatics. The first example was the pyrolysis of naphthalene at 1000 °C in an argon stream [58, 59]. The naphthalene skeleton is a monomer of the C_{60} structure. Fullerenes are formed by dehydrogenative coupling reactions. Primary reaction products are polynaphthyls with up to seven naphthalene moieties joined together. Full dehydrogenation leads to both C_{60} as well as C_{70} in yields less than 0.5%. As side products, hydrofullerenes, for example $C_{60}H_{36}$, have also been observed by mass spectrometry. Next to naphthalene, the bowl-shaped corannulene and benzo[*k*]fluoranthene were

also used as precursors to C_{60} [60]. Fullerene synthesis by laser pyrolysis is possible using benzene and acetylene as carbon sources [61]. Soot-free C_{60} has been produced in the liquid phase of an aerosol precursor of soot at 700 °C [62]. The precursor soot aerosol, a high temperature stable form of hydrocarbon, was produced by pyrolysis of acetylene at atmospheric pressure in a flow tube reactor. Further pyrolysis-based methods for the generation of fullerenes include CO_2-laser pyrolysis of small hydrocarbons such as butadiene and thermal plasma dissociation of hydrocarbons [63].

1.3.4 Generation of Endohedral Fullerenes

Since fullerenes are hollow molecules it should be possible to trap atoms inside the cage. Indeed, one week after the initial discovery of C_{60}, evidence for an endohedral lanthanum complex of C_{60} was obtained [64]. Laser vaporization of a graphite disk soaked in $LaCl_3$ solution produced an additional peak in the time-of-flight (TOF) mass spectrum due to La encapsulated by C_{60}. Evidence that endohedral complexes are so-formed came from "shrink-wrap" experiments showing that these complexes can lose, successively, C_2 fragments without bursting the cluster or losing the incorporated metal (Scheme 1.3) [65]. This is valid up to a certain limit, dictated by the ionic radius of the internal atom. For example, it was difficult to fragment past LaC_{44}^+ and impossible to go past LaC_{36}^+ without bursting the cluster [66].

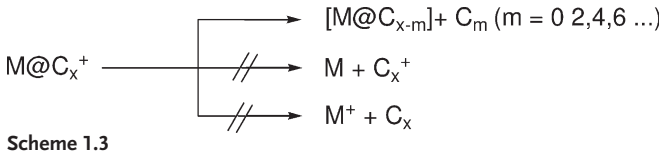

Scheme 1.3

To facilitate discussion of these somewhat more complicated fullerenes with one or more atoms inside the cage, a special symbolism and nomenclature was introduced [66]. Thereby the symbol @ is used to indicate the atoms in the interior of the fullerene. All atoms listed to the left of the @ symbol are located inside the cage and all atoms to the right are a part of the cage structure, which includes heterofullerenes, e.g. $C_{59}B$. A C_{60}-caged metal species is then written as M@C_{60}, expanded as "metal at C_{60}". The corresponding IUPAC nomenclature is different from the conventional M@C_n representation. IUPAC recommend that M@C_n be called [*n*]fullerene-*incar*-lanthanum and should be written *i*MC_n [4].

The production of endohedral fullerene complexes in visible amounts was first accomplished by a pulsed laser vaporization of a lanthanum oxide–graphite composite rod in a flow of argon gas at 1200 °C [66]. In this procedure, the newly formed endohedrals, together with empty fullerenes, sublime readily and are carried away in the flowing gas, depositing on the cool surfaces of the apparatus. This sublimate contains the complexes La@C_{60}, La@C_{74} and La@C_{82} (Figure 1.9). Among these, the endohedral molecule La@C_{82} exhibits an extra stability. It can

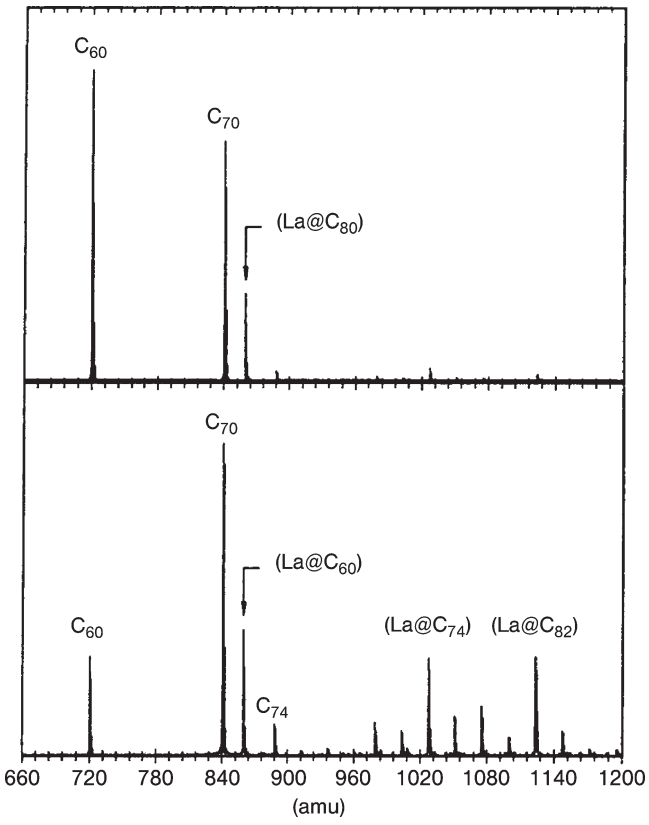

Figure 1.9 FT-ICR mass spectrum of hot toluene extract produced by laser vaporization of a lanthanum oxide–graphite composite rod [66].

be dissolved in toluene or carbon disulfide and exposed to air. The smaller lanthanum fullerenes are less stable and do not survive a hot extraction with toluene on air. The laser vaporization technique was also successful for the production of yttrium fullerenes such as $Y@C_{60}$, $Y@C_{70}$ and $Y_2@C_{82}$ in addition to $Y@C_{82}$ [67].

Along with laser vaporization methods, endohedral fullerene complexes can also be produced by arc vaporization of graphite impregnated with various metal oxides [66, 68–73] or rare earth metal carbides [74]. The yield of the lanthanofullerene $La@C_{82}$, for example, increases by a factor of 10 when, instead of metal-oxide-, metal-carbide-enriched composite graphite rods are used to generate soot [74]. More recent developments in the generation and characterization of endohedral metallofullerenes have been extensively reviewed by Shinohara [75, 76] and Nagase et al. [77]. In general, the endohedral complexes $M_n@C_{82}$ ($n = 1–3$) are the most abundant in the toluene or carbon disulfide extracts. However, metals, encapsulated in C_{60}, C_{74}, C_{76}, C_{80}, C_{84} and even in heterofullerenes such as $C_{79}N$ [78] have also been generated [75–77]. Endohedral complexes of inter alia La, Y, Sc, Ce, Pr, Nd, Sm, Eu, Gd, Tb, Dy, Ho, Er Tm, Yb and Lu, and also of Ca, Sr, Ba and Ti, can be prepared

[75–77]. The interior of C_{82}, approximately 8 Å in diameter, can readily accommodate three rare earth trivalent ions, which have average diameters of 2.06 to 2.34 Å [69]. The yield of dimetallo- or trimetallofullerenes depends on the metal-to-carbon ratio, whereas higher yields of multiple metal species are obtained by a higher metal content in the composite. Significantly, metallofullerenes encaged by C_{60} generally exhibit a very low abundance within most solvent-extracts, although empty C_{60} is the most abundant fullerene generated by the usual production methods. Possible reasons for this phenomenon are [72]: (1) $M@C_{60}$ fullerenes are unstable and destroyed upon exposure to air or moisture; (2) $M@C_{60}$ fullerenes are insoluble in organic solvents; and (3) the $M@C_{60}$ fullerenes are not preferably formed by this production method.

Interestingly, $M_n@C_{82}$ fullerenes are the most abundant, although empty C_{82} is not a dominant species formed under normal conditions. The fact that C_{80}, which in the empty case is an open shell system and therefore very unstable, also efficiently encapsulates rare earth metals, to form stable endohedrals $M_2@C_{80}$, suggests, that the electronic structure of the fullerene shell is dramatically influenced by the central metals. This, conversely, may be one reason for the possible instability of $M@C_{60}$. ESR studies on $M@C_{82}$ (M = Sc, Y, La) demonstrate that the metals are in the +3 oxidation state, [68, 73, 79] which leaves the fullerene in the trianionic state. This finding is corroborated by cyclic voltammetry studies on HPLC purified $La@C_{82}$ [80]. The cyclic voltammogram of dark green dichlorobenzene solutions of $La@C_{82}$ shows one reversible oxidation peak, the oxidation potential of which is approximately equal to that of ferrocene, implying that the complex is a moderate electron donor and therefore an oxygen-stable molecule. In addition, five reversible reductions are observed, showing that $La@C_{82}$ is a stronger electron acceptor than empty fullerenes, with the first reduction potential being especially low lying. These finding can be interpreted with the proposed molecular orbital diagram (Figure 1.10).

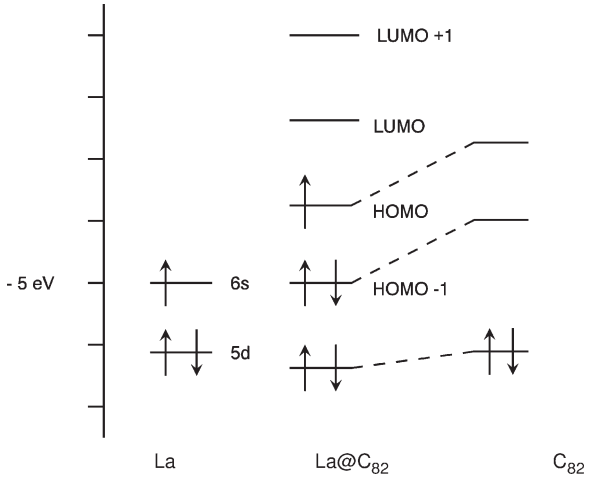

Figure 1.10 Schematic molecular orbital diagram of $La@C_{82}$ [80].

The removal of the radical electron corresponds to the first oxidation process. The resulting cation should be diamagnetic. The first reduction is relatively easy, because filling of the HOMO leads to the closed shell species $La@C_{82}^-$. Theoretical calculations predicted that the location of the lanthanum within the cage is off-center, which allows a stronger interaction with carbon atoms of the fullerene sphere [81–83].

Dynamic circular motion of the metal atoms within $La_2@C_{80}$ the cage has been investigated by NMR spectroscopy [77, 84, 85]. Synchrotron X-ray diffraction, ^{13}C NMR and ultra-high vacuum scanning tunneling microscopy (UHV-STM) studies also demonstrate the encapsulation of the metal atoms by the carbon cage [75, 76]. The metal atoms are not in the center of the fullerene cage but very close to the carbon cage, indicating a strong metal–cage interaction. Further electronic properties of endohedral metallofullerenes, such as redox behavior, have been investigated by cyclic voltammetry [75, 76, 86]. Various exohedral chemical functionalizations of endohedral metallofullerenes such as $La@C_{82,}$ $Pr@C_{82}$ and $Gd@C_{82}$ have been carried out [87, 88]. The endohedral metallofullerene $Gd@C_{82}$ is considered to be a promising agent for magnetic resonance imaging (MRI) due to the high spin state of the encapsulated ion [89].

Major drawbacks of the above synthesis methods are their low yields, typically < 0.5%, and the formation of multiple endohedral fullerene isomers. This makes it difficult to perform detailed studies of their properties and to use them for practical applications. In the regard the preparation of endohedral fullerenes such as $Sc_3N@C_{80}$ stands out [90]. The presence of small quantities of N_2 in a fullerene reactor allowed the synthesis of new endohedral fullerenes, such as the trigonal-planar Sc_3N unit encased in the high-symmetry, icosahedral C_{80}. The exact structure of $Sc_3N@C_{80}$ was determined by X-ray crystal structure analysis. ^{13}C NMR spectroscopic investigations revealed that, at room temperature, the Sc_3N unit is free to move in the C_{80} cage and so only two signals for the C-atoms in C_{80} are observed. This C_{80} isomer (Figure 1.11) is a third icosahedral fullerene, alongside C_{20} and C_{60}, and has an unstable and antiaromatic ground-state open-shell structure as an

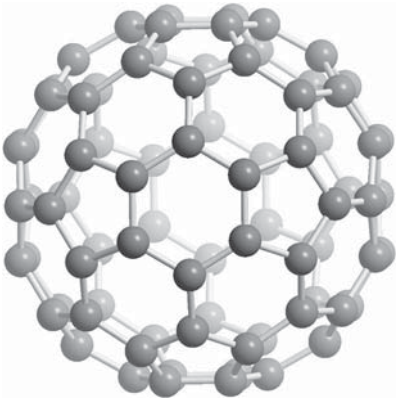

Figure 1.11 Icosahedral C_{80} cage of $Sc_3N@C_{80}$.

empty cage and has not yet been isolated. For $Sc_3N@C_{80}$, the cage is stabilized by six negative charges, which results in aromaticity [91]. Next to $Sc_3N@C_{80}$ a whole new family of stable endohedral fullerenes encapsulating trimetallic nitride clusters, $Er_xSc_{3-x}N@C_{80}$ ($x = 0$–3), has been generated [90, 92]. This 'trimetallic nitride template' process generates significant quantities of product, containing 3–5% $Sc_3N@C_{80}$. Also, the endohedral fullerene $Sc_3N@C_{78}$ was prepared and completely characterized [93]. Exohedral modification of $Sc_3N@C_{80}$ using Diels–Alder chemistry has been carried out [94]. Encapsulation has even been achieved of Sc_3N by the fullerene C_{68}, which does not obey the isolated pentagon rule [95], and by a C_{80} with D_{5h} symmetry [96].

Although electropositive metals afford endohedral complexes with fullerenes during their formation in macroscopic quantities, this is not the case with helium, the buffer gas used for the fullerene synthesis. Of 880 000 fullerene molecules generated by the arc-vaporization method only one was shown to contain a helium atom [97]. Conversely, mass spectrometry studies showed that an intact empty fullerene can be penetrated by the noble gas atoms He and Ne [98–104]. For this purpose singly and multiply charged C_x^{n+} fullerene molecules ($x = 60, 70$; $n = 1$–3) are shot through a stationary noble gas atmosphere in a molecular beam experiment. The resulting $M@C_{60}^+$ species show the "shrink-wrap" behavior with retention of M and successive elimination of C_2 (Scheme 1.3) that is typical for endohedral complexes. Upon reduction of $He@C_{60}^+$ the neutral complex $He@C_{60}$ can be obtained, which has a finite lifetime of > 90 μs [101]. This is further evidence that the noble gas is physically trapped inside the fullerene cage. The endohedral complex $He@C_{60}$ is the first noble gas–carbon compound.

To investigate the properties of endohedral noble gas fullerene compounds it is necessary to increase the fraction of the molecules occupied. This has been achieved by heating C_{60} or C_{70} in a noble gas atmosphere at high pressures (e.g. 2700 bar) and temperatures (e.g. 600 °C) [105, 106]. Next to helium, neon, argon, krypton and xenon have also been incorporated into fullerenes by this method. Mole fractions of $X@C_{60}$ and $X@C_{70}$ (X = Ne, Ar, Kr, Xe) in the range 0.04–0.3% have been estimated by mass spectrometry [106, 107]. In addition, beam implantation methods have been used for the generation of endohedral noble gas fullerenes [108]. Since the abundance of C_{60} and C_{70} with four ^{13}C atoms is high enough to interfere with the peaks of $He@C_{60}^+$ and $He@C_{70}^+$ it is difficult to measure the extent of helium incorporation by mass spectrometric methods. The use of ^3He, however, allows one to record ^3He NMR spectra since ^3He has spin = ½. The ^3He NMR spectra of $^3He@C_{60}$ and $^3He@C_{70}$ show that the incorporation fraction is about 0.1% [105, 106]. ^3He NMR spectroscopy can also be used to measure the shielding environment inside the fullerene cavity. The ^3He nuclei encapsulated in C_{60} and C_{70} are shielded by 6.3 and 28.8 ppm respectively relative to free ^3He [105, 106]. These shieldings indicate significant diamagnetic ring currents in C_{60} and very large ones in C_{70}. ^3He NMR spectroscopy of endohedral He complexes of a whole series of fullerenes [109–111], including exohedral fullerenes adducts [112–119], charged fullerenes [120, 121] heterofullerenes [122] and other cluster modified fullerenes [123], is a very powerful method for investigating the magnetic properties of carbon cages

[124]. It can be also very important for determining the number of isomers of higher fullerenes of regioisomers of exohedral fullerene adducts and for carrying out mechanistic investigations on the escape of the endohedral guest and reversible addition reactions [125]. The ^{129}Xe NMR spectrum of Xe@C_{60} has also been reported [126].

Since the penetration of a noble gas atom through a six-membered ring would afford a very high activation energy, the formation of X@C_{60} or X@C_{70} (X = noble gas) must be accompanied by the breaking of at least one bond of the fullerene core. A window mechanism has been proposed to explain the penetration of noble gases into the fullerene cages [127]. The energetics of opening both the [6,6]-bond and the [5,6]-bond have been calculated [127]. A comparison of the reaction coordinates for the processes of breaking a [6,6]-bond in the C_{60} singlet ground state and a [5,6]-bond in the triplet state reveals an energetic preference for the latter process. The opening of one [5,6]-bond leads to the formation of a nine-membered ring, which is expected to be large enough for atoms to pass in or out. After the thermal breaking of a bond the fullerene, either filled with a noble gas atom or empty, can reform by closing the opened bond or it can react further, via another irreversible pathway, to form degraded fullerenes. Degradation products have indeed been found by the synthesis of X@C_{60} or X@C_{70} [105, 106].

Another striking development with endohedral fullerenes was the synthesis of N@C_{60}, the first example of encapsulation of a reactive nonmetal atom [128–132]. It is particularly surprising that the enclosed nitrogen exists as a single atom and no bonding to the fullerene framework is apparent. The fullerene therefore represents a trap for extremely reactive atomic nitrogen. This occurs because curvature results in the inner surface of the fullerene cage being inert, whilst the outer surface is distinguished by high reactivity [133]. The formation of a covalent bond with the enclosed N-atom, which has a half-filled p-shell (three unpaired electrons) and so displays minimal electron affinity, would lead to a distinct rise in the strain energy of the total system. Thanks to the absence of relaxation mechanisms, the lowest ESR linewidths observed occur in the spectra of N@C_{60} [134]. The wavefunction of the enclosed N atom is influenced by subsequent exohedral adduct formation with one or more addends [134]. This is caused by the altered cage structure of the adducts. The analogous complexes N@C_{70} and P@C_{60} are made similarly to N@C_{60}, by bombarding a thin layer of fullerene on a cathode with energy-rich N- or P-ions, respectively [135, 136].

1.3.5
Total Synthesis Approaches

Fullerene generation by vaporization of graphite or by combustion of hydrocarbons is very effective and certainly unbeatable what facile production in large quantities is concerned. However, total synthesis approaches are attractive because (a) specific fullerenes could be made selectively and exclusively, (b) new endohedral fullerenes could be formed, (c) heterofullerenes and (d) other cluster modified fullerenes could be generated using related synthesis protocols.

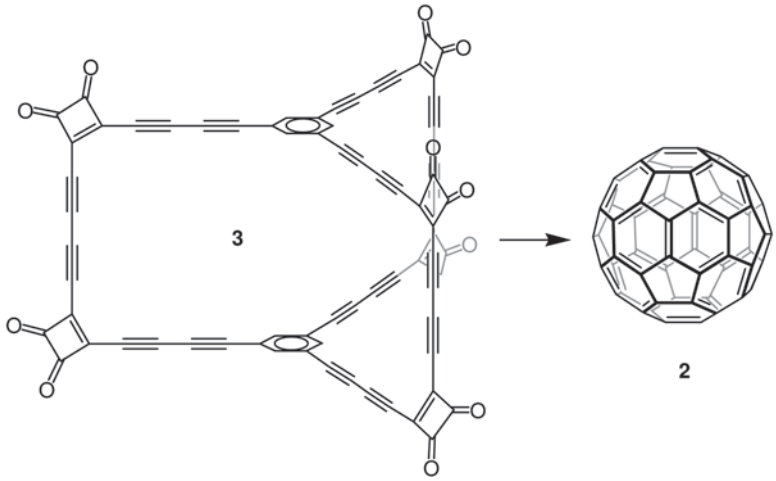

Scheme 1.4 Conversion of cyclophane **3** into C_{60} in the gas phase in laser desorption mass spectrometry.

Three approaches for rational syntheses of fullerenes have been developed. The first approach is the zipping up of fullerene precursors [137–144]. Carbon-rich acetylenic spherical macrocycles such as **3** (Scheme 1.4) may function as precursors of C_{60} and even its endohedral metal complexes in a process analogous to the coalescence annealing of mono- and polycycles with sp-hybridized C-atoms [139] during gas-phase formation of fullerenes from evaporated graphite [137]. Indeed **3** is effectively converted into $C_{60}H_6$ and C_{60} ions in the gas phase in laser desorption mass spectrometry experiments [138]. Related cyclophanes involving pyridine – instead of benzene moieties – are precursors for the conversion into the heterofullerene $C_{58}N_2$ in a mass spectrometer [143].

The second approach is based on the idea of synthesizing bowl-shaped hydrocarbons in which curved networks of trigonal C-atoms map out the same patterns of five- and six-membered rings as those found on the surfaces of C_{60} and/or the higher fullerenes [145–152]. An example for such an "open geodesic polyarene" is circumtrindene (**5**), generated by flash-vacuum pyrolysis (FVP) of trichlorodecacyclene **4** (Scheme 1.5) [152]. Circumtrindene represents 60% of the framework of C_{60}.

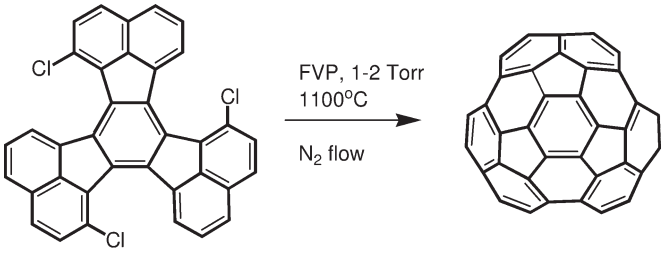

Scheme 1.5 Synthesis of circumtrindene (**5**), representing 60% of C_{60}.

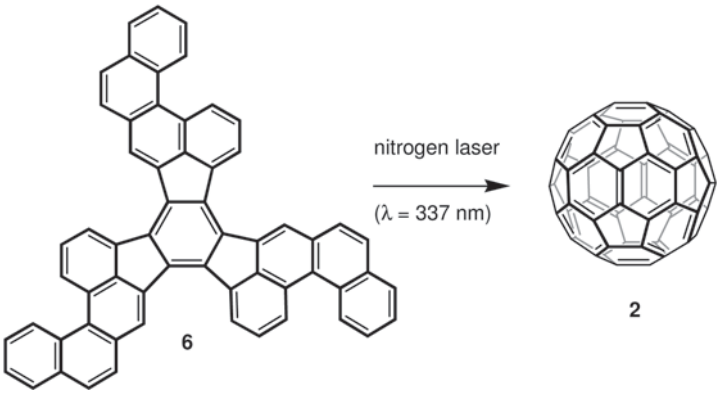

Scheme 1.6 Generation of C_{60} by cyclodehydrogenation of polyarene **6**.

All 60 C-atoms of C_{60} are incorporated in the $C_{60}H_{30}$ polycyclic aromatic hydrocarbon (PAH) **6**, for which an efficient synthesis was developed [153]. Laser irradiation of **6** at 337 nm induces hydrogen loss and the formation of C_{60}, as detected by mass spectrometry (Scheme 1.6). Control experiments with ^{13}C-labeled material and with the $C_{48}H_{24}$ homologue of **6** verified that the C_{60} is formed by a molecular transformation directly from the $C_{60}H_{30}$ PAH and not by fragmentation and recombination in the gas phase.

In a third approach substituents were removed from a preformed dodecahedrane cage. In this way the synthesis of [20-I_h]fullerene was possible in the gas phase [154]. However, extensions of this approach to syntheses of fullerenes consisting of 60 or more C-atoms are conceptually very difficult.

1.3.6 Formation Process

Even though fullerenes are significantly destabilized with respect to graphite [155], they are readily formed out of a chaotic carbon plasma at about 3000 K. A thermodynamically controlled pathway leading to highly symmetric fullerenes can be ruled out. If the fullerene formation would be thermodynamically controlled, then, for example, the yield of C_{70}, which is more stable than C_{60}, [156, 157] should be much higher than found in extracts from graphitic soot. The toluene extract of soot, obtained by carbon vaporization, contains predominantly C_{60} followed by C_{70}. The ratio C_{60}:C_{70} is about 85 : 15 [25]. Therefore kinetic factors must govern the fullerene generation. [60-I_h]Fullerene is the most stable C_{60} isomer. Furthermore, the energy per carbon of [60-I_h]fullerene is much lower than any isomer of C_{58} and C_{62}. Locally, [60-I_h]fullerene is in a deep potential well and, if once formed from clustering carbon, it is chemically inert. This explains the much lower abundance of the higher fullerenes. One reason for the stability of C_{60} is that it obeys the "isolated pentagon rule" (IPR), which allows only fullerenes in which all pentagons are completely separated from each other by hexagons [158, 159]. [60-I_h]Fullerene is at the same

time the smallest possible fullerene that obeys the IPR. The next most stable isomer of C_{60} has two pairs of adjacent pentagons and has been calculated to be 2 eV higher in energy [160]. These stability considerations already imply that if clusters smaller than C_{60} are formed they will undergo further reactions in the plasma and if those being a little bit larger than C_{60} are formed, for example C_{62}, they can be stabilized by loss of small fragments (C_2) and rearrangements, leading to the survivor [60-I_h]fullerene. Analogous processes should be valid for the higher fullerenes.

A mechanism for fullerene generation [38, 88, 161–167] by vaporization of graphite has to consider three major stages: (1) the vaporization itself and the nature of the initially formed intermediates; (2) the structure of the growing clusters and (3) the annealing to the fullerenes. The first step in the fullerene generation by evaporation of graphite is the formation of carbon atoms, as shown experimentally by $^{12}C/^{13}C$ isotope scrambling measurements [168–170]. The distribution of ^{13}C among the C_{60} molecules follows exactly Poisson statistics. The next step is the clustering of the carbon atoms. The smaller clusters are linear carbon chains or carbon rings. This was concluded by mass spectrometry studies of carbon clusters generated by laser desorption [171–174] and is supported by calculations [175, 176]. If reactive components are added to the buffer gas during the graphite vaporization such early intermediates can be quenched and the fullerene formation is suppressed (Scheme 1.7) [19, 177–179]. Laser desorption of graphite in the presence of H_2 allowed the mass spectrometric observation of polyynes [19]. Similar rod-shaped molecules, the dicyanopolyynes NC-$(C\equiv C)_n$-CN (n = 3–7), are obtained in high yields upon vaporization of graphite in an He/$(CN)_2$ atmosphere (Scheme 1.7) [178]. Obviously, in both cases irreversible additions of H atoms and CN-radicals to the ends of linear carbon chain intermediates are occurring. If Cl_2 is added to the

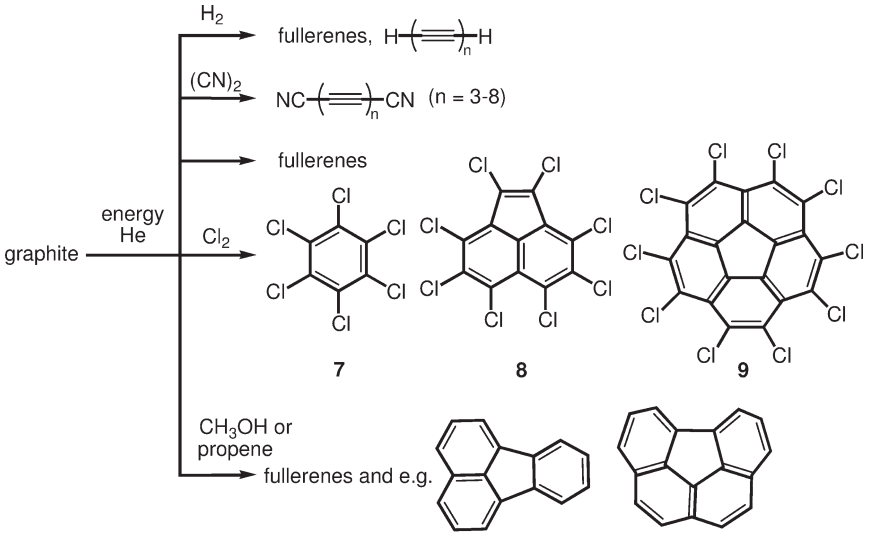

Scheme 1.7

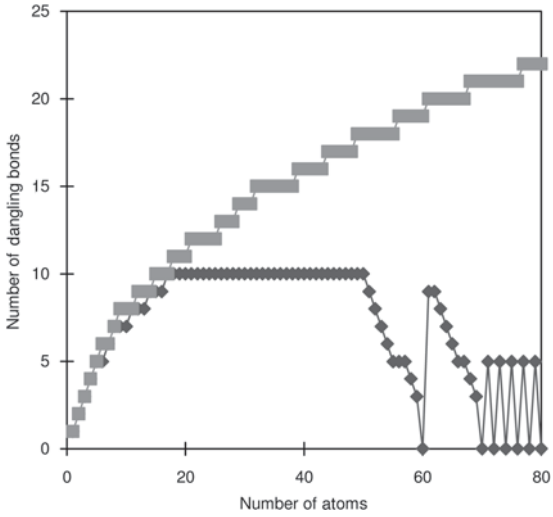

Figure 1.12 Number of dangling bonds in the best possible structure for a graphitic sheet with (*top*) all hexagons, compared to (*bottom*) those which obey the IPR, as a function of the number of atoms in the sheet [181].

buffer gas, instead of linear chains, perchlorinated cyclic compounds are found in the toluene extract of the soot (Scheme 1.7). The amount of fullerenes in the extract is < 5%. Each carbon framework of the cyclic compounds **7–9** represents a part of the C_{60}-structure. Thereby, it is remarkable that, already, structures containing pentagons, for example, the decachlorocorannulene **9** are formed. Polyaromatic hydrocarbons (PAHs) such as **10** and **11** can be isolated, if the vaporization of graphite is carried out in an atmosphere of He/propene or He/methanol (Scheme 1.7). Systems with a similar carbon framework are suggested to be present as intermediates during the formation of fullerenes in benzene flames [51]. However, it can not be concluded from the quenching experiments alone whether clusters with structures like **7–11** are indeed predominant intermediates in the fullerene formation, since the presence of reactive species influences the growth process. The mechanisms of fullerene formation by graphite evaporation and by combustion or pyrolysis of naphthalene are thought to be different.

Graphitic sheets as intermediates for cluster sizes of 30 or more C-atoms are proposed in the "pentagon road" model [162, 180, 181]. Thereby it is emphasized that the growth process of the graphitic sheet follows a low energy path by minimizing the number of dangling bonds. This can be achieved by the introduction of pentagons accompanied by a curling process (Figure 1.12). A complete closure to a fullerene reduces the number of dangling bonds to zero. This model also takes into account that high energy adjacent pentagon structures are avoided and also explains (1) the need for an elevated temperature for effective fullerene formation, because prior to a further growth an annealing process leads to an isolated pentagon network and (2) the role of the buffer gas as well as the pressure dependence on the

fullerene yield, because the helium concentration controls the diffusion of the C_n species from the hot into cooler zones of the plasma. Higher buffer gas pressures lead to an increase in concentration of reactive C_n, which causes the annealing process to be not competitive with the cluster growth. During annealing, the formation of a low energy structure obeying the IPR could be accomplished inter alia by the Stone–Wales rearrangement (Scheme 1.8) [182]. This is a concerted process, involving a Hückel four-center transition state.

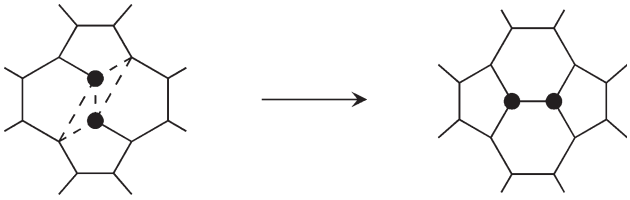

Scheme 1.8

Graphitic sheets, however, are not detectable in the carbon-plasma by ion chromatography (IC) [162, 174, 183–185]. This method provides a means for separating carbon cluster ions with different structures because the reciprocal of the ion mobility is proportional to the collision cross-section. Several species C_n^+ with different structures coexist and their relative amount depends on the cluster size. Small clusters C_n^+ ($n < 7$) are linear. In the range $n = 7$–10 chains as well as monocycles coexist. The clusters C_{11}^+–C_{20}^+ are exclusively monocycles and the range between C_{21}^+ and C_{28}^+ is characterized by planar mono- and bicyclic systems. The first three-dimensional structure is detected at C_{29}^+ and the first fullerenes appear at C_{30}^+ and dominate from C_{50}^+. Therefore, the growth pattern for carbon in the plasma starting from atoms is linear → monocyclic rings → polycyclic rings and finally → fullerenes.

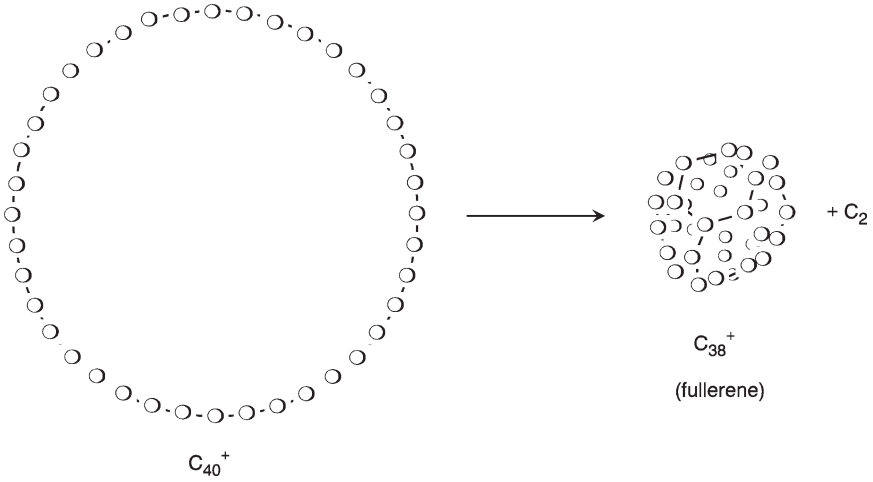

Figure 1.13 Generation of the fullerene C_{38}^+ by collision induced heating of the macrocycle C_{40}^+.

If such mixtures of ions, generated by laser desorption of graphite, are annealed by collisions, predominantly monocyclic rings are formed upon isomerization of the initial structures. At very high collision energies, isomerization to fullerenes occurs. The fullerenes C_n^+ so-obtained carry enormous internal energy, which can be dissipated by the cleavage of C_1- or C_3- (for odd n) or C_2-fragments (for even n) (Figure 1.13). From drift experiments, the more rings the initial structure contains the smaller the ring barrier is to rearrangement to a fullerene [162]. Tricyclic or tetracyclic isomers rearrange readily to form fullerenes, while bicyclic and monocyclic rings are significantly slower.

Another important series of experiments has shown, by ion-cyclotron-resonance (ICR) studies, that monocyclic carbon rings can coalesce very efficiently to fullerenes (Scheme 1.9) [139]. The carbon rings are obtained by laser desorption of carbon oxide $C_n(CO)_{n/3}$ precursors, out of which, upon loss of CO, the cyclo[n]carbons C_{18}, C_{24} and C_{30} are generated. Fullerene formation proceeds via collisions of positively charged cluster ions C_n^+ with the corresponding neutrals. In the positive ion mode, reactions between cations and neutral molecules of the cyclo[n]carbons lead to fullerene ions. Remarkably, the cyclocarbons C_{18} and C_{24} predominantly lead, via

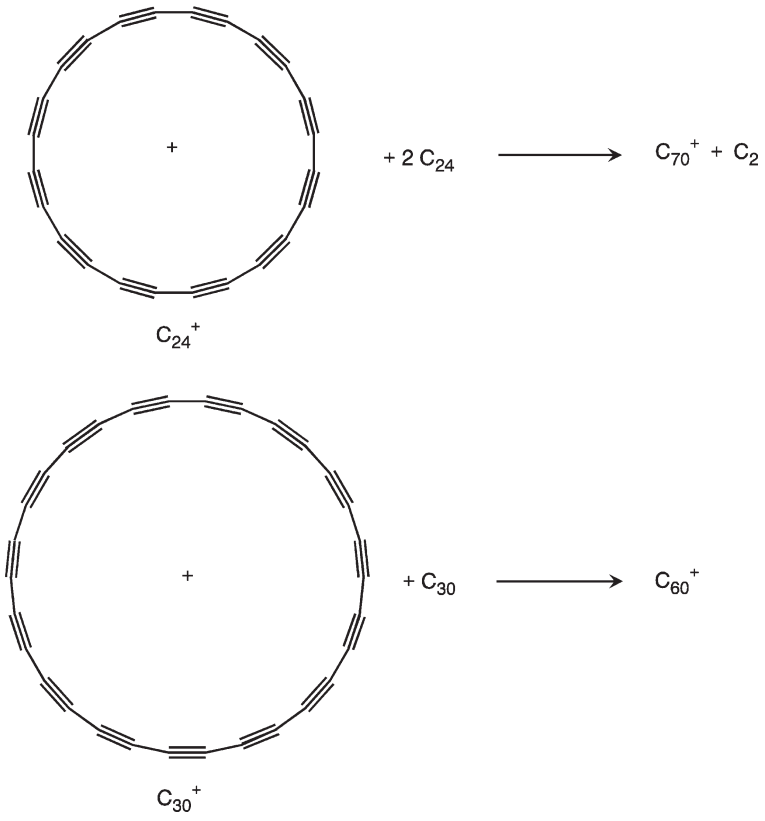

Scheme 1.9